Available online at www.sciencedirect.com

SCIENCE DIRECT®

Experimental Neurology 193 (2005) 394–410

Experimental Neurology

www.elsevier.com/locate/yexnr

04-3030

Embryonic radial glia bridge spinal cord lesions and promote functional recovery following spinal cord injury

Koichi Hasegawa[1,2], Yu-Wen Chang[1], Hedong Li, Yana Berlin, Osamu Ikeda[3], Noriko Kane-Goldsmith, Martin Grumet*

W. M. Keck Center for Collaborative Neuroscience, 604 Allison Road, Rutgers, State University of New Jersey, Piscataway, NJ 08854-8082, USA

Received 13 August 2004; revised 18 November 2004; accepted 10 December 2004
Available online 3 March 2005

Abstract

Radial glial cells are neural stem cells (NSC) that are transiently found in the developing CNS. To study radial glia, we isolated clones following immortalization of E13.5 GFP rat neurospheres with v-myc. Clone RG3.6 exhibits polarized morphology and expresses the radial glial markers nestin and brain lipid binding protein. Both NSC and RG3.6 cells migrated extensively in the adult spinal cord. However, RG3.6 cells differentiated into astroglia slower than NSC, suggesting that immortalization can delay differentiation of radial glia. Following spinal cord contusion, implanted RG3.6 cells migrated widely in the contusion site and into spared white matter where they exhibited a highly polarized morphology. When injected immediately after injury, RG3.6 cells formed cellular bridges surrounding spinal cord lesion sites and extending into spared white matter regions in contrast to GFP fibroblasts that remained in the lesion site. Behavioral analysis indicated higher BBB scores in rats injected with RG3.6 cells than rats injected with fibroblasts or medium as early as 1 week after injury. Spinal cords transplanted with RG3.6 cells or dermal fibroblasts exhibited little accumulation of chondroitin sulfate proteoglycans (CSPG) including NG2 proteoglycans that are known to inhibit axonal growth. Reduced levels of CSPG were accompanied by little accumulation in the injury site of activated macrophages, which are a major source of CSPG. However, increased staining and organization of neurofilaments were found in injured rats transplanted with RG3.6 cells suggesting neuroprotection or regrowth. The combined results indicate that acutely transplanted radial glia can migrate to form bridges across spinal cord lesions in vivo and promote functional recovery following spinal cord injury by protecting against macrophages and secondary damage.

Keywords: Radial glial cells; Neuroprotection; Neurofilaments; Proteoglycans; BBB; Neuron–glia interaction; Macrophages

Introduction

Important advances have been made in understanding conditions that influence survival and regrowth of neurons following injury to mature CNS tissue. These include neurotrophic factors to promote survival and growth of neurons, embryonic neural tissues to provide cellular scaffolds to facilitate neuronal regrowth, and neutralization of inhibitors (Bregman, 1998; Jones et al., 2001; Schwab, 2002). Another approach to repair neural damage is replacement of lost cells, in particular neurons, which can be obtained by differentiating neural stem cells (Gage, 2000; McKay, 1997). These approaches are well suited for problems like Parkinson's disease where replacement of lost dopaminergic cells can yield significant recovery of function (Kim et al., 2002). However, many other neurons, for example, supraspinal neurons

* Corresponding author. Fax: +1 732 445 2063.
E-mail address: mgrumet@rci.rutgers.edu (M. Grumet).
[1] These authors contributed equally to the manuscript.
[2] Present address: Mie University, Department of Neurosurgery, Mie, Japan.
[3] Present address: Kamitsuga Sogo Hospital, Department of Orthopedic Surgery, Tochigi, Japan.

0014-4886/$ - see front matter © 2004 Elsevier Inc. All rights reserved.
doi:10.1016/j.expneurol.2004.12.024

whose axons are damaged in spinal cord injury, have their cell bodies in locations (e.g., motor cortex) that are quite far from the site of injury in the spinal cord; such neurons, which may be lost following damage to their axons, are difficult to replace but it may be possible to regenerate their axons under appropriate conditions before they die (Rosenzweig and McDonald, 2004; Schwab, 2002; Silver and Miller, 2004). Thus, there is a need for other strategies to protect neurons and promote their regrowth across sites of injury.

Radial glia appear transiently during development spanning CNS tissues where they serve as scaffolds to support migration of neurons (Hatten and Heintz, 1995) and their processes (Brittis et al., 1995; Norris and Kalil, 1991). Recent observations made with a highly polarized rat cell line called C6-R suggested that radial glial-like cells are able to migrate extensively in the white matter and infiltrate into lesioned neural tissues (Friedlander et al., 1998; Hafidi et al., 2004; Hormigo et al., 2001a). Like radial glia (Hatten, 1993), C6-R cells promoted migration of neurons and neuronal processes both in vitro and in vivo (Hormigo et al., 2001b). However, C6-R, which was derived from C6 glioma, formed tumors when transplanted into the contused spinal cord (Hasegawa and Grumet, 2003). Therefore, it was of interest to identify alternative sources of radial glia lacking tumorigenicity.

Hatten and colleagues have pioneered methods to isolate and study cerebellar radial glia in vitro, but these cells are highly unstable loosing their bipolar morphology in the absence of neuronal contact in vitro and in the mature nervous system in vivo (Hunter and Hatten, 1995). Recent studies have provided convincing evidence that most or all embryonic radial glia initially are neural stem cells (NSC) or are restricted precursors derived from them that give rise to neurons early during embryogenesis and to glia at later stages (Anthony et al., 2004; Gotz et al., 2002; Noctor et al., 2002). Given that viral introduction of v-myc has enabled isolation of NSC lines (Villa et al., 2000), we isolated, following introduction of v-myc (Li et al., 2004), clones from E13–15 rat cortices where NSC and radial glia are prevalent. An initial set of clones exhibited properties common to radial glia and NSC including markers and bipolar morphology, and they supported neuronal migration in vitro (Li et al., 2004). In this paper, we describe a similar clone isolated from a GFP-expressing rat (Ito et al., 2001) called RG3.6. These fluorescently tagged cells also share properties with radial glia but maintain their radial glial-like properties longer than acutely isolated NSC. Interestingly, they migrate extensively in the white matter tracts of the spinal cord in uninjured rats as well as in the contused rat spinal cord forming a continuum across spinal cord lesions. RG3.6 transplantation enhanced neurofilament organization in spinal cord tissue following injury and animals transplanted with RG3.6 showed improved behavioral recovery.

Materials and methods

NSC and radial glial-like cell clone RG3.6

Neurospheres prepared from E13.5 GFP rat embryo forebrains were dissociated by trypsinization after 2 days (Li et al., 2004). This yielded a population of cells that were nearly all nestin+ consisting of a combination of NSC and progenitors that will be referred to here as primary NSCs. For immortalization, the primary NSCs were cultured on laminin-coated substrates for 2 days and infected with PK-VM-2 retrovirus (from Dr. Evan Snyder) as described (Li et al., 2004; Villa et al., 2000). After 4–5 days in selection in 200 μg/ml G418 (Invitrogen), individual cells were cloned at limiting dilution in 96-well plates. 36 clones were obtained and upon passage nine were selected that exhibited polarized morphology and contained only brain lipid binding protein (BLBP) (Feng and Heintz, 1995) positive cells but were negative for NeuN (Chemicon, Temecula, CA) and GFAP (Li et al., 2004). Of these, four clones including RG1.9, RG3.6, RG3.7, and RG4.7 were selected for further analysis. For differentiation, passage (P) 7 of RG3.6 cells and P7 NSCs were each cultured on laminin-coated coverslips in fibroblast growth factor2 (FGF2; 10 ng/ml, BD Biosciences) containing serum-free DMEM/F12 medium for 1 day, then the medium was replaced with culture medium lacking FGF2, including 1% fetal bovine serum (FBS) for 6 days, and the cultures were fixed and immunostained. All cell culture products were from Invitrogen, Carlsbad, CA, and all chemicals were from Sigma-Aldrich, St. Louis, MO, unless specified otherwise.

Immunofluorescence of cells in culture

RG3.6 neurospheres were dissociated and plated on coverslips coated with 20 μg/ml laminin. Cells were fixed with 4% paraformaldehyde for 15 min at room temperature and washed with PBS. Cells were incubated with one of the following primary antibodies in 10% normal goat serum and 0.3% Triton X-100 in PBS for 2 h at room temperature: mouse monoclonal anti-nestin at 1:40 (Developmental Study Hybridoma Bank, Iowa City, IA), rabbit polyclonal anti-BLBP at 1:1000 (from Dr. Nathaniel Heintz), rabbit polyclonal anti-GFAP at 1:200 (R401), mouse monoclonal antibody TuJ1 (recognizes βIII tubulin) at 1:200 (Chemicon, Temecula, CA), and mouse monoclonal anti-GalC at 1:50 (from Dr. Randall D. McKinnon). After washing, cells were incubated with appropriate secondary antibodies at 1:200 (Molecular Probes, Eugene, OR) for 1 h at room temperature: Alexa 568-conjugated goat anti-mouse IgG and Cy5-conjugated goat anti-rabbit IgG (Jackson Immunoresearch, West Grove, PA). Cells were washed, nuclei were labeled with Hoechst 33342 at 1:2000, and coverslips were mounted with Gel/Mount (Biomedia, Foster city, CA). Images were acquired on a Zeiss Axiophot microscope and were analyzed in Adobe Photoshop 6 or 7. The total number of cells was determined by counting the total number of nuclei that were

stained with Hoechst dye. A cell was identified as positive for a cell type-specific marker (TuJ1, Nestin or GFAP) if the red signal stained both its processes and the outline of the nucleus. Percentage of positive cells was calculated at 1 and 2 weeks after differentiation.

Cell transplantation

A total of 18 adult female Sprague–Dawley (SD) rats (Taconic, Germantown, NY) weighing 200–250 g were used to study the intact spinal cord. Animals were anesthetized with intraperitoneal injection of pentobarbital (35 mg/kg, Abbott Laboratories, IL) and laminectomies were performed to expose thoracic segments T9–10. RG3.6 or NSC cells were dissociated with trypsin into single cells in DMEM + F12 medium, resuspended in the same medium, and diluted to a density of 0.5–2 × 10^5 cells/μl. Cells were injected slowly during a period of 10 min into ventral column of T10 using a sterile glass tip with a diameter of 50 μm connected to a 5-μl Hamilton syringe. After injections, the muscle and skin were closed separately. Cefazolin (25 mg/kg, VWR International, Pittsburgh, PA) was administered for 7 days after surgery to prevent infection. Cyclosporin A (Sandoz Pharmaceuticals, East Hanover, NJ) was administered subcutaneously at a dose of 10 mg/kg body weight throughout the survival period and animals were euthanized at different time points (1 week, n = 6; 2 weeks, n = 6; and 4 weeks, n = 6). To study differentiation, we quantitated GFP-labeled cells that were nestin or GFAP positive 4 weeks after implantation of RG3.6 or GFP-NSC into intact spinal cord. Tissue processing and immunostaining were described previously (Hormigo et al., 2001b), and nuclei were labeled with Hoechst. More than 300 GFP+ cells were counted for each animal. To quantitate marker staining, projections of confocal stacks were used to identify GFP+ cells that were positive for nestin or GFAP (see Fig. 4), and colocalization for each cell was verified by scanning through the confocal stacks. Two observers scored expression levels of each Hoechst+ GFP+ cell as: ++, strong positive cells; +, weak positive cells; −, negative cells; or unidentified cells. For cerebellar transplants, P3 rat pups were rendered unconsciousness by chilling the animals at 4°C for 1–2 min, a small incision was made in the skin, and a Hamilton syringe needle was lowered gently through the incision to a position just beneath the meninges. 2.5 × 10^4 RG3.6 cells were injected slowly on each side of the cerebellum. After withdrawing the needle, the skin incision was closed with 7–0 silk suture (Ethicon). The animal was warmed to 35.5°C and returned to the litter. They were euthanized after 3 days.

Contusion injury and cell transplantation

A total of 46 adult female SD rats weighing 200–250 g were used in this study including 16 to optimize cell dosing using cells at 0.5–2 × 10^5/μl. Rats were anesthetized and the spinal cord was exposed by laminectomy on T9–10. Contused spinal cords were produced by dropping a 10.0-g rod onto the exposed spinal cord from a height of 12.5 mm using the MASCIS impactor (Constantini and Young, 1994). After injections, muscles and skin were closed separately. Cyclosporin A was administered subcutaneously at a dose of 10 mg/kg body weight throughout the survival period. Animals were euthanized 6 weeks after the contusion injury and spinal cords were treated as described (Roonprapunt et al., 2003).

Experiment 1

A total of 4 μl (2 μl at the center of the contusion site and 1 μl each at 2 mm rostral and caudal sites from the center) of RG3.6 cells (2 × 10^5/μl) or vehicle medium (DMEM + F12) was injected (n = 8 for RG3.6, n = 4 for medium).

Experiment 2

Procedures were the same as experiment 1, except that GFP rat skin fibroblasts (0.5 × 10^5/μl) were injected instead of medium (n = 10 for RG3.6, n = 10 for GFP fibroblasts). For experiment 1, half of the spinal cords were cut sagittally at 20 μm as cryostat sections and the other half were cut horizontally at 7 μm as paraffin sections. To quantify the number of neurofilament-stained axons at the epicenter of contusion site, axons were counted in every sixth section for cryostat sections and in every fifteenth section for paraffin sections. Experiments 1 and 2 were performed by different surgeons. For experiment 2, all the spinal cords were cut sagittally at 20 μm as cryostat sections, and dorsal and ventral NF staining was measured.

Locomotor recovery for experiments 1 and 2 was assessed weekly using the 21-point BBB score (Basso et al., 1996a,b) by two separate BBB scoring teams that were unaware of experimental treatments. BBB scores of 0–7 represent hindlimb movements with no weight support; a score of 8 signifies sweeping or plantar placement without weight support, while a score of 9 indicates plantar placement weight support in stance only with no plantar stepping. A score of 10 indicates occasional weight supported plantar steps without forelimb coordination while a score of 11 requires consistent weight-supported plantar stepping with no forelimb–hindlimb coordination. Scores of 12 and 13 represent frequent to consistent weight supported plantar steps with occasional forelimb–hindlimb coordination. Rutgers University Animal Use and Care Committee approved all animal procedures used in the studies.

Histological procedures

Animals were euthanized with an intraperitoneal injection of sodium pentobarbital (50 mg/kg, Besse Medical Supply/ASD Specialty Healthcare, Louisville, KY), followed by transcardial perfusion with 4% paraformaldehyde in 0.1 M

phosphate buffer after vascular washout with PBS. The spinal cords were removed, post-fixed overnight in the same fixative, cryoprotected with 20% sucrose overnight, and embedded in OCT compound (Fisher Scientific, Pittsburgh, PA). Horizontal (for transplantation in intact spinal cord) or sagittal (for transplantation in injured spinal cord) sections were cut at 20 μm with a cryostat (Hacker) and mounted on Superfrost Plus Microscope Slides (Fisher brand). Cerebella were fixed similarly except they were embedded in 3% agarose and 100-μm sections were cut with a Vibratome. For immunostaining, slides were blocked with 10% normal goat serum/0.3% Triton X-100 in PBS for 2 h at room temperature and incubated overnight at 4°C with one of the following primary antibodies: rabbit polyclonal anti-GFAP at 1:200, mouse monoclonal anti-nestin at 1:40, mouse monoclonal antibody CS56 (recognizes chondroitin sulfate) at 1:400 (Sigma-Aldrich, St. Louis, MO), rabbit polyclonal antibody against NG2 proteoglycan (Levine and Card, 1987) at 1:500 (from Dr. Joel M. Levine), mouse monoclonal antibody ED1 (recognizes activated macrophages) at 1:300 (Serotec, Raleigh, NC), and mouse monoclonal anti-neurofilament at 1:500 (Clone N52, Sigma-Aldrich, St. Louis, MO). Sections were washed with PBS and incubated with appropriate secondary antibodies at 1:400 dilution for 1 h at room temperature: Alexa 568-conjugated goat anti-rabbit IgG, Alexa 568-conjugated goat anti-mouse IgG, Alexa 488-conjugated goat anti-mouse IgG, Cy5-conjugated goat anti-rabbit IgG (Jackson Immunoresearch, West Grove, PA). Sections were washed with PBS and counterstained with Hoechst 33342 and mounted with Gel/Mount or ProLong antifade mounting medium (Molecular Probes). Image analysis was performed using Zeiss 510 confocal laser scanning microscope (LSM). Intact spinal cords were imaged with a Cool Snap Pro camera (Media Cybernetics) using a Zeiss Stemi II microscope equipped with fluorescence optics. Luxol Fast Blue staining, which stain myelin blue, was performed as described (Carson, 1997; Luna, 1968) and images were acquired using bright field on a Zeiss Axiophot.

Quantification of immunostained sections

Quantification of spinal cord area immunolabeled for CS56, NG2, and NF was performed using Zeiss 510 LSM confocal software. Two parasagittal sections within 200 μm of the midline were used for each animal. Tiled images composed of thirty 10× images with a frame size of 2700 μm × 9200 μm were employed to cover ~9 mm length in sagittal sections centered around the injury site. All staining was performed under the same conditions and images were acquired with invariant parameters using the Zeiss 510 LSM system. Staining intensity thresholds for each antibody were determined after all images were acquired to optimize the signal to noise ratio for each antibody. Over the range of intensities from 0 to 255, thresholds were set at 50 for CS56, 60 for NG2, and 80 for NF. Areas with intensities higher than thresholds were recorded and normalized to the total areas measured to

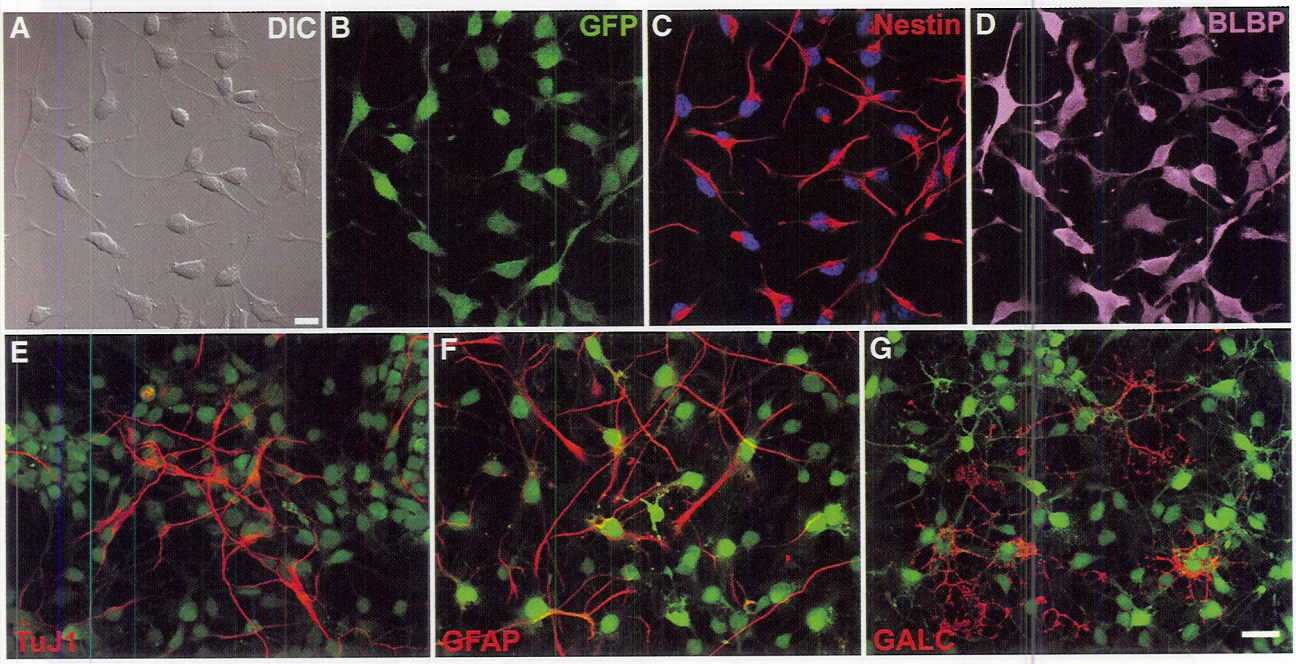

Fig. 1. RG3.6 cells exhibit features of both radial glial and neural stem cells. Confocal microscopic images of the same field of RG3.6 cells showing cellular morphology by differential interference contrast (DIC) (A), GFP (B), nestin (red) revealing radial morphology and nuclei (DAPI, blue) (C), and radial glial marker BLBP (D). Note colocalization in all cells. After withdrawal of bFGF and incubation in 1% fetal bovine serum and 10 μM retinoic acid for 3 days, RG3.6 gave rise to cells expressing the neuronal marker TuJ1 (E), astrocyte marker GFAP (F), and oligodendrocytes marker GALC (G). Scale bar is 20 μM in A–D and 40 μM in E–G.

obtain the percent of labeling. Regions of meninges and dorsal root ganglion were excluded. Quantification of NF staining in cryosections was performed similarly except the tiled images consisted of 6 images covering the injury center. 1-mm lengths of dorsal and ventral white matter were outlined as indicated in Fig. 9, excluding meninges, dorsal root ganglia, cysts, and central fibroblast masses where cysts typically form. White matter regions, which were identified by light microscopy and verified in certain cases by staining with Luxol Fast Blue (Carson, 1997; Luna, 1968), were followed from regions that were well preserved into the lesion site. For paraffin sections, the numbers of NF+ filaments in mid-sagittal sections were counted along the dorsal–ventral axis at the center of the injury site.

Statistical analysis

Data in each analysis are expressed as the mean ± SEM. Differences among the means were evaluated by Fisher's protected least significant difference (PLSD). $*P < 0.05$; $**P < 0.01$; $***P < 0.001$.

Results

Generation and characterization of immortalized radial glial-like clone RG3.6

We recently generated clones from embryonic rat cortex by immortalizing them with v-myc retrovirus (Villa et al., 2000) that exhibited properties of radial glia (Li et al., 2004). In order to visualize radial glia in vivo, we derived another set of clones from E13.5 GFP rat cortical neurospheres. After selection with G418, individual clones were isolated and most including RG3.6 had a bipolar morphology (Figs. 1A and B). Among the clones that were generated, many were found to express the radial glial markers BLBP, nestin (Figs. 1C and D), and vimentin (not shown). Four representative clones were tested for their behavior following transplantation into adult spinal cord and all migrated robustly along the rostral–caudal axis in white matter tracts. Among these clones, we selected RG3.6 for detailed examination since it showed extensive migration and no tendency for mass

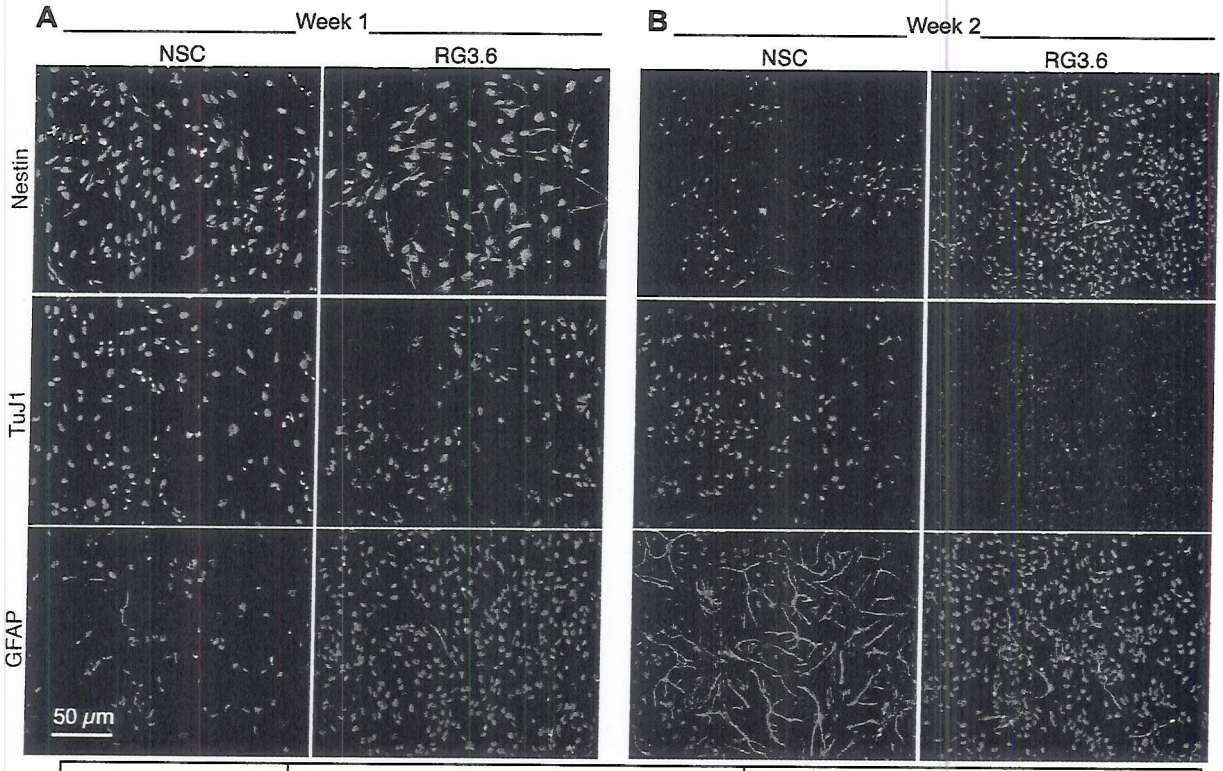

C

	Week 1		Week 2	
	NSC	RG3.6	NSC	RG3.6
Nestin	60.4% (n=197)	97.0% (n=98)	41.6% (n=505)	44.8% (n=2019)
TuJ1	23.5% (n=174)	0.5% (n=227)	21.0% (n=536)	2.0% (n=1837)
mGFAP	4.7% (n=137)	0.2% (n=443)	50.0% (n=580)	20.6% (n=2004)

Fig. 2. Comparison of differentiation between NSC and RG3.6 cells in vitro. Nestin, TuJ1, and GFAP staining (red) of NSC and RG3.6 cells after 1 (A) and 2 (B) weeks in differentiation medium. Note the increase in GFAP staining for the NSC at 2 weeks indicating glial differentiation. Nuclei were stained with DAPI (blue) and the numbers and percent of positive cells in each case are shown in the table (C).

formation in spinal cord. The group of clones exemplified by RG3.6 cells express markers for radial glia (Figs. 1C and D) but not for neurons (NeuN and β-III tubulin), oligodendrocytes (O4), and astrocytes (GFAP).

Considering evidence that radial glia are NSC that can give rise to neurons and glia (Anthony et al., 2004; Gotz et al., 2002), we examined the differentiation of RG3.6 cells in vitro. Upon withdrawal of FGF2 from the culture medium and addition of 1% FBS plus 10 μM retinoic acid, cells differentiated within 3 days into neurons (Fig. 1E), astrocytes (Fig. 1F), and oligodendrocytes (Fig. 1G), with astrocytes being the most prevalent differentiated cells obtained. The addition of FBS during differentiation increased the proportion of astrocytes and decreased the proportion of oligodendrocytes, while more oligodendrocytes were obtained without serum or FGF2, and more neurons with retinoic acid (data not shown) as expected (Mabie et al., 1997; Takahashi et al., 1999). RG3.6 also shares these properties with clone L2.3 (Li et al., 2004) as well as the ability to support neuronal migration in vitro (data not shown). Following transplantation into early postnatal cerebellum, RG3.6 cells coaligned with nestin+ radial glia (data not shown). Thus, RG3.6 cells exhibited morphological, molecular, and developmental properties of radial glia (Noctor et al., 2002).

RG3.6 cells differentiate slower than rat cortical NSCs

One rationale for introducing v-myc into NSCs was to inhibit their ability to differentiate (Villa et al., 2000). To determine whether this was true, we compared the differentiation of RG3.6 cells with non-infected NSCs. After 1 week of differentiation, the NSC showed a marked decrease in the intensity of nestin staining (Fig. 2A) as well as in the percentage of nestin+ cells by comparison to RG3.6 cells (Fig. 2C). Within 2 weeks in the absence of FGF2, most NSCs differentiated into astrocytes expressing GFAP and ~20% differentiated into neurons expressing TuJ1 (Figs. 2A–C). Cell counts confirmed that RG3.6 cells differentiated into fewer GFAP+ cells and much fewer TuJ1+ neurons than the NSC (Fig. 2C). At 2 weeks, the nestin+ RG3.6 cells were typically bipolar like radial glia in contrast to the more

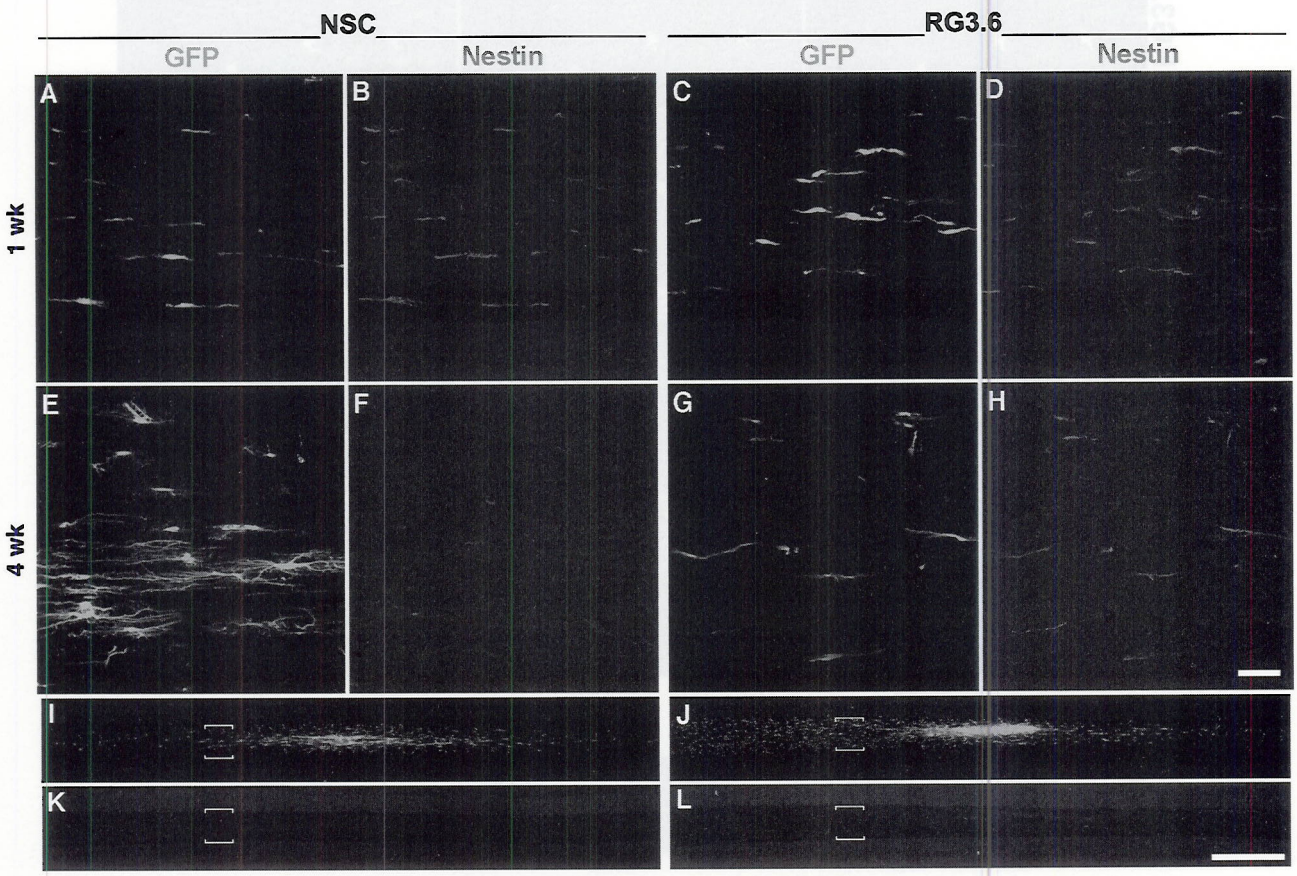

Fig. 3. Differences in morphology and differentiation between NSC and RG3.6 cells in vivo. NSC (A, B, E, F, I, and K) and RG3.6 cells (C, D, G, H, J, and L) at 1 (A–D) and 4 (E–H) weeks after transplantation into the normal spinal cord. At 1–2 weeks, both NSC and RG3.6 cells have bipolar morphologies, and most cells are still nestin-positive (red). At 4 weeks after transplantation, some NSCs have multipolar processes and most are negative or only weakly positive for nestin. In contrast, most RG3.6 cells are still bipolar and are strongly positive for nestin. Note the extensive migration of GFP+ cells in the white matter (M–P); panels O and P are corresponding fields stained with anti-neurofilament (red). Panels I and K represent bracketed regions in M and N, respectively, that are >1 mm from the implantation site. Scale bars = 50 μm (A–H); 1 mm (I–L). (For interpretation of the references to colour in this figure legend, the reader is referred to the web version of this article.)

astrocytic morphology observed for the NSCs (Fig. 2B). Another v-myc-transduced clone called RG4.7 behaved similarly to RG3.6 upon differentiation (data not shown). These results indicate that viral introduction of v-myc inhibits differentiation of NSCs and allows persistence of many cells with a radial glial phenotype.

The differentiation of these cells in the adult spinal cord was compared to evaluate their potential use for transplantation following spinal cord injury. One week following transplantation into normal adult spinal cord, RG3.6 and NSC migrated extensively along the rostral–caudal axis in the white matter (Figs. 3A–D) and much less migration was observed into grey matter as described previously for C6-R radial cells (Hormigo et al., 2001b). Both RG3.6 cells and GFP-NSCs were nestin+ and exhibited bipolar morphologies with cells in white matter aligned along the rostral–caudal axis. By 4 weeks following transplantation, most of the GFP-NSCs did not stain for nestin in contrast to the RG3.6 cells, most of which still expressed nestin. Moreover, at 4 weeks, the RG3.6 cells retained their bipolar morphology while GFP-NSCs often exhibited complex morphologies characteristic of more differentiated cells (Figs. 3E–G). Many of these complex cells exhibited multiple processes that were GFAP+ (Fig. 4), suggesting that many GFP-NSCs differentiated into astrocytes. It is noteworthy that GFP expression persisted robustly in transplanted cells with nearly every nestin+ cell being GFP+, in contrast to the normal adult spinal cord where there are very few nestin+ cells (Fig. 3). Low magnification montages of both NSC (Figs. 3I and K) and RG3.6 (Figs. 3J and L) showed extensive migration along the rostrocaudal axis primarily in white matter.

A previous study showed that after implantation into the rodent spinal cord, nestin+ NSC gradually differentiated

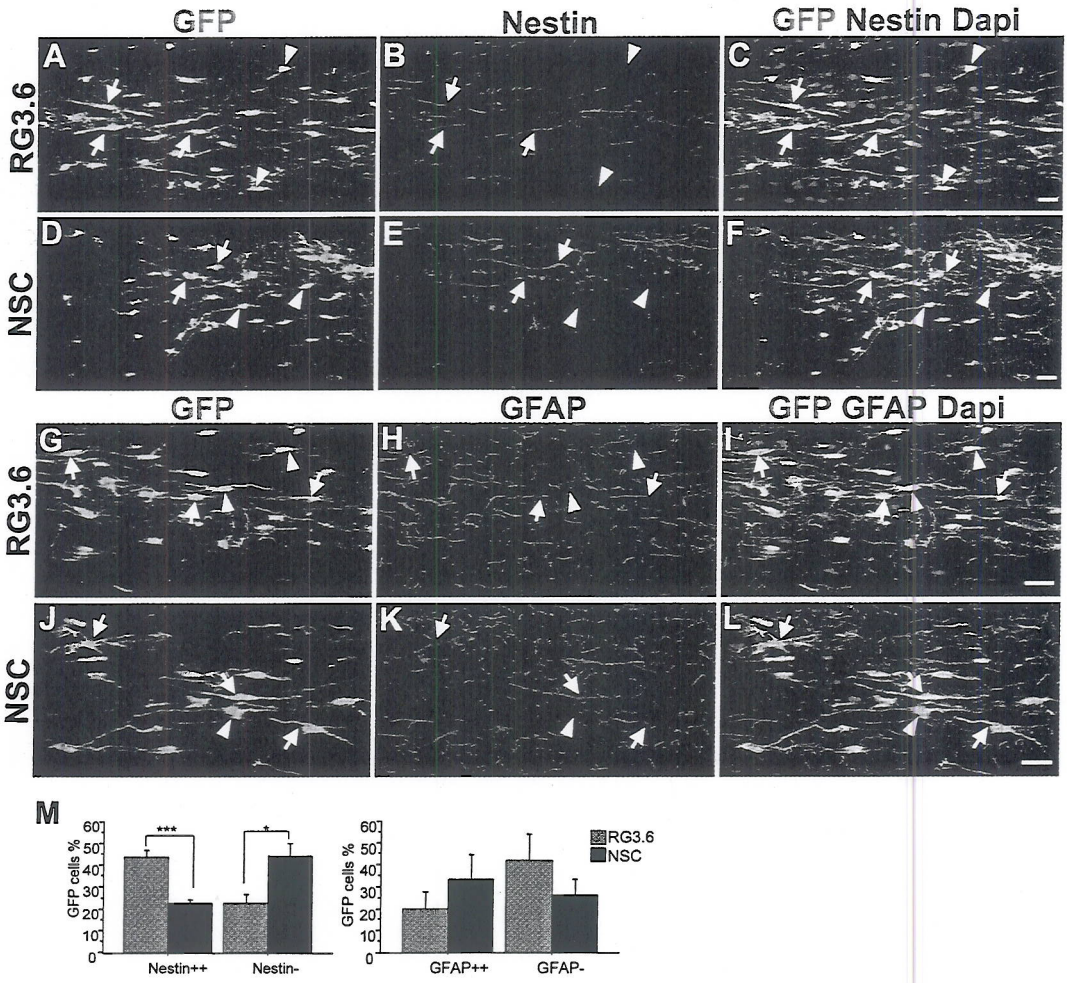

Fig. 4. Differentiation of RG3.6 is slower than NSC in normal spinal cord. GFP (A, D, G, and J) fluorescence was compared with staining for nestin (B and E) or GFAP (H and K) 4 weeks after transplantation of RG3.6 cell (A–C and G–I) and NSC (D–F and J–L). Both RG3.6 and NSC survive and migrate in the white matter. We counted non-differentiated GFP+/nestin++ cells (arrows) and differentiated GFP+/nestin− cells (arrowheads) (A–F), and astrocytes as GFP+/GFAP++ cells (arrows) and GFP+/GFAP− cells (arrowheads) (G–L) in different rats injected with RG3.6 and NSC cells. C, F, I, and L are merged confocal images <1 mm from the injection site. Scale bar is 20 μm. Quantitative results (M) show more RG3.6 cells are nestin++ and more NSCs are GFAP++. Percentages do not sum to 100% because weakly positive cells were omitted because their percentages did not differ significantly. Data shown are means ± SEM with 3 rats per group (*$P < 0.05$, ***$P < 0.001$).

primarily into astrocytes (Cao et al., 2001). To compare the differentiation of NSC with RG3.6 in vivo, we analyzed the percent of Hoechst+/GFP+ transplanted cells that expressed nestin (Figs. 4A–F) or GFAP (Figs. 4G–L). We quantified the percent of GFP+ cells that did not differentiate as the fractions that were nestin++ (strong positive, arrows in Fig. 4) and found twice as many nestin++ cells with RG3.6 than with NSCs (Fig. 4M). In a complementary manner, the percent of nestin− cells (arrowheads) was higher for the NSCs than with RG3.6. This analysis yielded statistically significant differences and was fairly straightforward given that there was little endogenous nestin staining in the adult spinal cord. We also quantified the percent of GFAP++ cells as a measure of cell differentiation since most cells that differentiated did so along the astrocytic lineage. However, this was much more complex given the widespread expression of GFAP by endogenous astrocytes in the spinal cord. Nevertheless, we did find similar patterns of differentiation insofar as a higher percentage of NSCs was strongly GFAP++ and a higher percentage RG3.6 cells was GFAP− (Fig. 4M).

Transplanted RG3.6 cells bridge spinal cord lesions and promote functional recovery

Contusion Experiment 1: RG3.6 vs. medium control

Immediately following contusion of adult rat spinal cords with the MASCIS Impactor, GFP-labeled RG3.6 cells or medium was injected at 3 positions (2 μl at the center of injury and 1 μl each at 2 mm rostral and caudal). Gross anatomical analysis after 6 weeks showed shrinkage of spinal cords injected with medium only (Fig. 5A). Initial experiments were performed to optimize cell dosing. Injection of RG3.6 at 2×10^5 cells/μl reduced the dramatic shrinkage in the spinal cord at the injury site (Fig. 5B) while shrinkage was found at lower doses. Fluorescence imaging

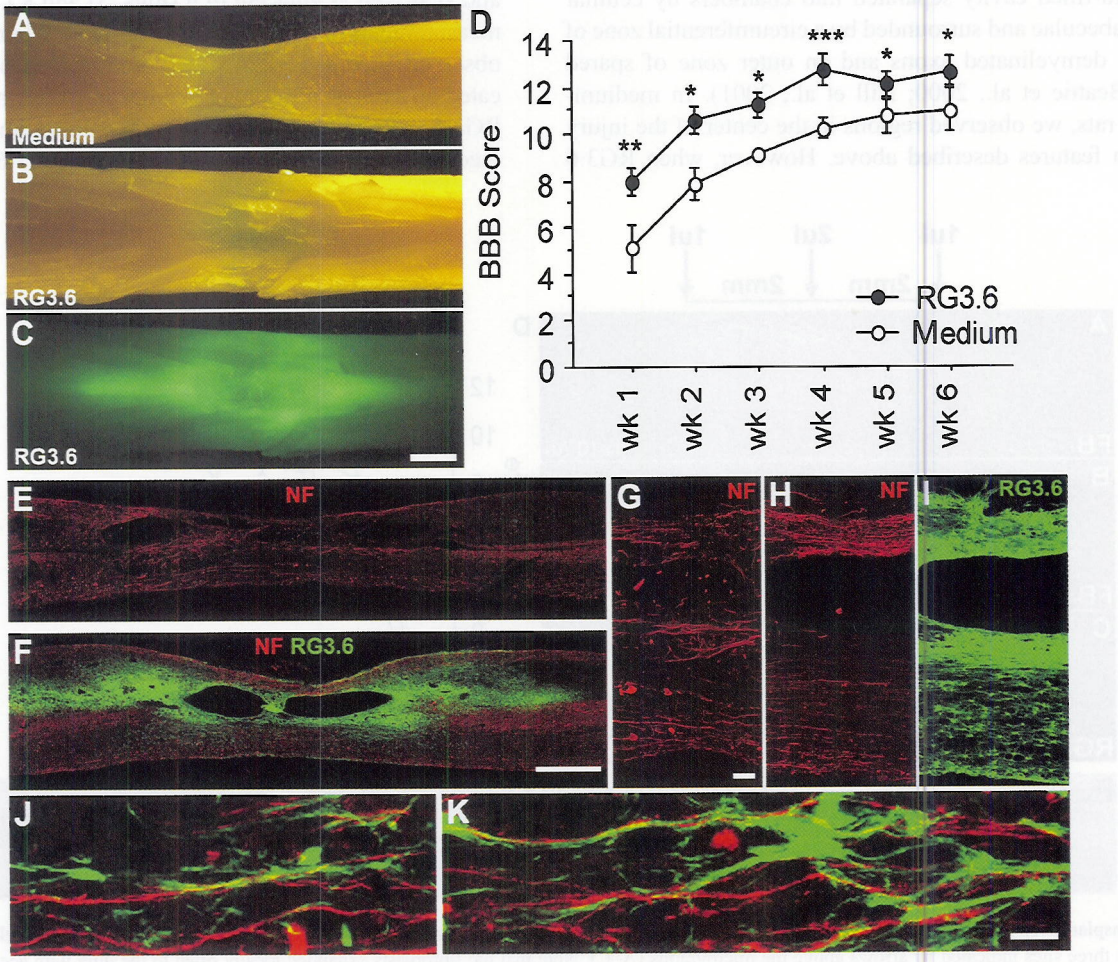

Fig. 5. Transplantation of RG3.6 cells improved tissue preservation and behavioral recovery. Whole mounts of spinal cords dissected from rats injected with medium (A) or RG3.6 cells (B and C) visualized by light (A and B) and fluorescence microscopy (C). BBB open field behavioral tests were performed weekly. RG3.6 (●) showed consistently higher scores than medium (○) transplanted group. $n = 8$ animals for RG3.6, $n = 4$ for medium. Data represent mean ± SEM ($^*P < 0.05$, $^{**}P < 0.01$, $^{***}P < 0.001$, ANOVA repeated measures). NF staining in sagittal sections of contused spinal cord injected with medium (E and G) or RG3.6 cells (F and H–K). Panels G and H are higher magnifications of the center of injury sites showing disorganized NF in medium-treated rats by comparison to the more longitudinally organized NF patterns in RG3.6-treated rats (panel I shows the RG3.6 cells corresponding to panel H). Panels J and K are high magnification images from regions adjacent to the center of injury. Scale bars = 1 mm in C and F, 100 μm in G and H, and 20 μm in J and K.

of the intact cords often showed GFP+ cells surrounding a central region with lower GFP intensity that is likely to represent cysts (Fig. 5C and compare to Figs. 5F and 6C). Remarkably, the RG3.6 cells were observed several millimeters from the injection sites, indicating they had migrated rostrally and caudally (Figs. 5C and F). In cell dosing studies, functional analysis indicated that there was a trend toward higher BBB scores when 1×10^5 cells/μl were used and a greater increase when 2×10^5 cells/μl were used (data not shown). BBB scores were significantly higher for the rats that received RG3.6 cells (2×10^5 cells/μl) than for those that received only medium (Fig. 5D). Interestingly, differences in BBB scores of >2 points were observed early following contusion (e.g., at 1 week RG3.6 = 8.000 ± 0.590 vs. medium = 5.123 ± 1.008), suggesting a protective effect on the spinal cord following contusive injury.

Following contusion to the rat spinal cord, there is extensive apoptosis and necrosis resulting in the formation of a fluid-filled cavity separated into chambers by cellular tissue trabeculae and surrounded by a circumferential zone of partially demyelinated axons and an outer zone of spared fibers (Beattie et al., 2000; Hill et al., 2001). In medium-injected rats, we observed regions in the center of the injury site with features described above. However, when RG3.6 cells were injected, these cells surrounded one or more cavities in the lesion site and appeared to migrate lon distances primarily along the rostral and caudal axis, most extensively into spared white matter regions (Fig. 5F). Moreover, we observed trabeculae in the injury site of the medium-treated rats (Figs. 5E and G) but not in rats injected with RG3.6 cells (Figs. 5F, H, and I). These trabeculae are thought to be formed by infiltrating cells after injury (Hill et al., 2001), and their absence in rats treated with RG3.6 cells suggests that the radial glia may interfere with the migration of other cells into the lesion site. Axons were often observed in a disorganized pattern in the lesion site of medium-injected rats perhaps growing among the trabeculae (Fig. 5G). In contrast, with RG3.6 transplants, nearly all NFs were aligned longitudinally in register with the orientation of the GFP+ radial glial cells and the NF staining in these regions was often fairly dense (e.g., in the dorsal region of Fig. 5H). The close association between axons and RG3.6 fibers was observed dorsal and ventral to the injury site (Figs. 5F, H, and I) as well as adjacent to it (Figs. 5J and K). Quantitative measurements of the numbers of NF+ filament bundles observed in mid-sagittal paraffin-embedded sections indicated on average 42% more bundles in cords implanted with RG3.6 cells (524 ± 30, $n = 3$) than cords implanted with medium (369 ± 22, $n = 3$). Thus, RG3.6 transplants

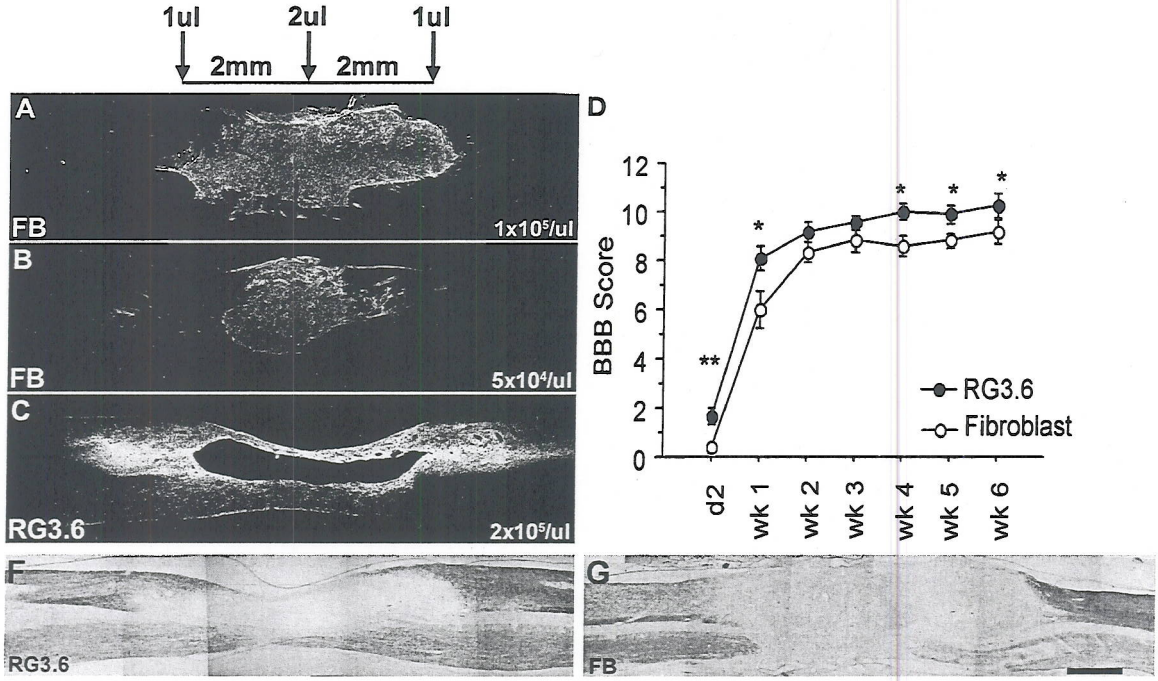

Fig. 6. Transplantation of RG3.6 cells improved behavioral recovery and myelin after injury. GFP fluorescence shows fibroblasts and RG3.6 cells 6 weeks after injection at three sites indicated by arrows above the micrographs (A–C). Note that the fibroblasts expanded locally often to the dura with accumulations that were dose-dependent (A vs. B). In contrast, RG3.6 cells migrate rostrocaudally and surrounded the cystic cavities that formed (C). BBB open field behavioral tests were recorded weekly for each animal (D). Statistically significant differences were observed at day 2 and several subsequent time points between the two groups with RG3.6 (●) showing consistently better performance than the fibroblast (○) transplanted group. $n = 10$ per group. Data represent means ± SEM (*$P < 0.05$, **$P < 0.01$, ANOVA repeated measures). Luxol Fast Blue staining showed better preservation of myelin in RG3.6 (F) than in fibroblast (G transplanted rats; panels F and G are from the same spinal cords shown in panels C and A, respectively. Note the continuity across the injury site of myelinated bridges with RG3.6 but not with fibroblasts. Scale bar = 1 mm. (For interpretation of the references to colour in this figure legend, the reader is referred to the web version of this article.)

improved tissue organization and behavioral recovery by comparison to medium controls.

Contusion Experiment 2: RG3.6 cells vs. fibroblasts

We next tested GFP fibroblasts as a cellular control using the same injection protocol (Fig. 6). Initial experiments were performed to optimize fibroblast cell dosing. 6 weeks after transplant using fibroblasts at 1–2 × 10^5 cells/μl, these GFP+ cells filled the lesion site and often formed bulges in the spinal cord that were not observed with similar numbers of RG3.6 cells. Reducing fibroblasts to 0.5 × 10^5 cells/μl reduced the bulging. Histological analysis confirmed that robust GFP fluorescence persisted in fibroblasts and RG3.6 cells, but the fibroblasts remained almost exclusively in the spinal cord injury site (Figs. 6A and B) as shown previously (Grill et al., 1997; Liu et al., 1999, 2002a; Tuszynski et al., 1994, 1996). In contrast, the RG3.6 cells surrounded the injection site and were observed several millimeter rostral and caudal, indicating they had migrated into spared white matter tracts where they were aligned along the rostral–caudal axis (Figs. 5F and 6C) as they did in the normal spinal cord (Figs. 3 and 4).

By 3 weeks following contusive injury to the rat spinal cord, cavities typically form in the injury site (Hill et al., 2001), but they were not observed with fibroblast implants as these cells filled the injury site (Figs. 6A and B). In contrast, RG3.6 cells surrounded the injury site and extended into adjacent spared tissue forming a continuum across the injury site at 6 weeks (Figs. 5F and 6C).

Besides differences in cell migration in the spinal cord, the larger size of the fibroblasts may contribute to the distention of the spinal cord as observed with fibroblasts implanted at 1–2 × 10^5 cells/μl but not with similar doses of radial glia (Figs. 6A and C). Because of potential complications of the mass effect with the fibroblasts that are larger in volume than the radial glia, fibroblasts were used at 0.5 × 10^5 cells/μl in the behavioral studies. Walking function was analyzed using BBB scores, which were consistently higher for rats that

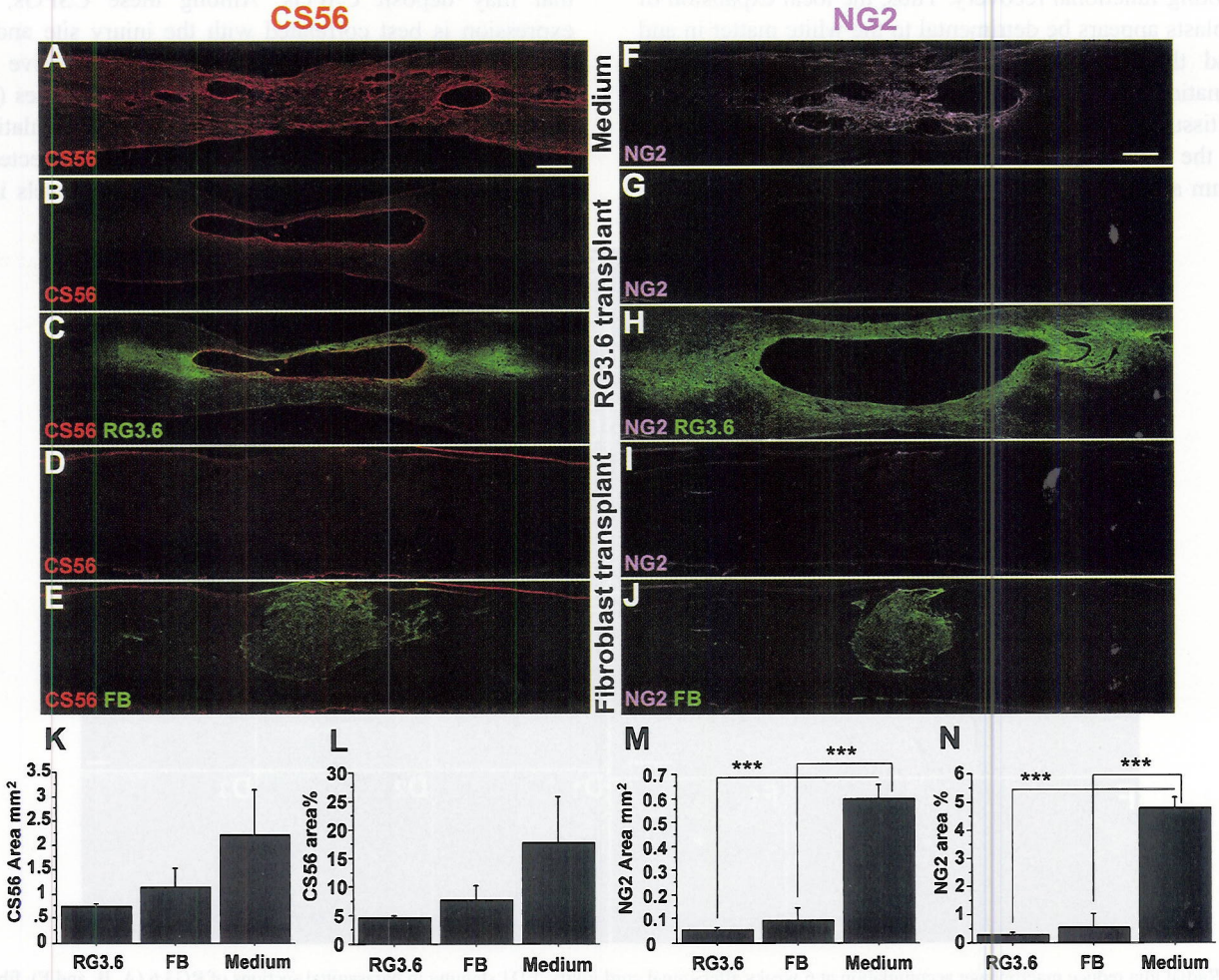

Fig. 7. Radial glia reduce deposition of CSPG and NG2 at 6 weeks after spinal cord injury. Parasagittal sections of control medium (A and F), RG3.6 (B, C, G, and H), and fibroblast (FB) (D, E, I, and J) treated groups were immunostained with monoclonal antibody CS56 (A–E) and anti-NG2 (F–J). 30 (10×) images were tiled (X: 10, Y: 3) to cover the injury site (9 mm × 3 mm) using Zeiss LSM software. Areas with intensity above threshold values for CS56 or NG2 were taken from each tile scan (K and M) and normalized to the total area of each sagittal spinal cord segment (L and N). Scale bar is 500 μM. Data represent means ± SEM with 3 rats per group (***$P < 0.001$).

received RG3.6 cells than those that received fibroblasts (Fig. 6D). The differences in BBB scores were small but significant with the largest differences observed at 7 days (RG3.6 = 8.111 ± 0.491 vs. fibroblast = 6.000 ± 0.775), too early to result from regeneration or sprouting (Bareyre et al., 2004), suggesting that RG3.6 cells protected the spinal cord from secondary injury.

Although implantation of various types of cells might improve recovery by simply replacing lost cells and preventing cord shrinkage, the results indicated a statistically significant improvement of the RG3.6 cells vs. controls (Figs. 5D and 6D), suggesting that RG3.6 cells had particular properties that were beneficial. Rats that received RG3.6 cell transplants exhibited preservation of some white matter both dorsal and ventral in the injury site that typically spanned across it (Fig. 6F). In contrast, there was little or no white matter preservation in the injury site with fibroblast transplants (Fig. 6G). Although fibroblasts were able to fill the lesion site and prevent spinal cord shrinkage, they were not as effective as the RG3.6 cells in promoting functional recovery. Thus, the local expansion of fibroblasts appears be detrimental to the white matter in and around the injury site (Fig. 6G). To explore potential explanations for the ability of the RG3.6 to preserve spinal cord tissue, we compared histological markers in tissues from the injured rats treated with RG3.6, fibroblasts, or medium alone.

RG3.6 cells inhibited accumulation of CSPG and macrophages following spinal cord injury

The early improvement in behavioral scores with RG3.6 cell transplants (Figs. 5 and 6) suggested that the spinal cord was being protected from secondary damage. Various factors associated with neural tissue damage including chondroitin sulfate proteoglycans (CSPG) are believed to inhibit cell adhesion and axonal growth (Davies et al., 1997; Grumet et al., 1993, 1996; Jones et al., 2002). Immunostaining with monoclonal antibody CS56 confirmed extensive deposits of CSPGs in the spinal cord following contusive injury (Fig. 7A). CSPG staining was present in the injury site in a trabecular pattern as well as in the walls surrounding the cysts. In contrast, there was much less CSPG deposition following transplantation of RG3.6 cells (Figs. 7B and C) or fibroblasts (Figs. 7D and E). Some weak CSPG staining was observed surrounding but not inside cysts that formed with RG3.6 transplants, suggesting that perhaps the radial glia prevented infiltration of other cells that may deposit CSPGs. Among these CSPGs, NG2 expression is best correlated with the injury site and may derive from several local sources including reactive astrocytes, oligodendrocyte precursors, and macrophages (Jones et al., 2002). We confirmed the enhanced accumulation of NG2 in and around the injury site of medium-injected rats (Fig. 7F), but NG2 was present at negligible levels in rats

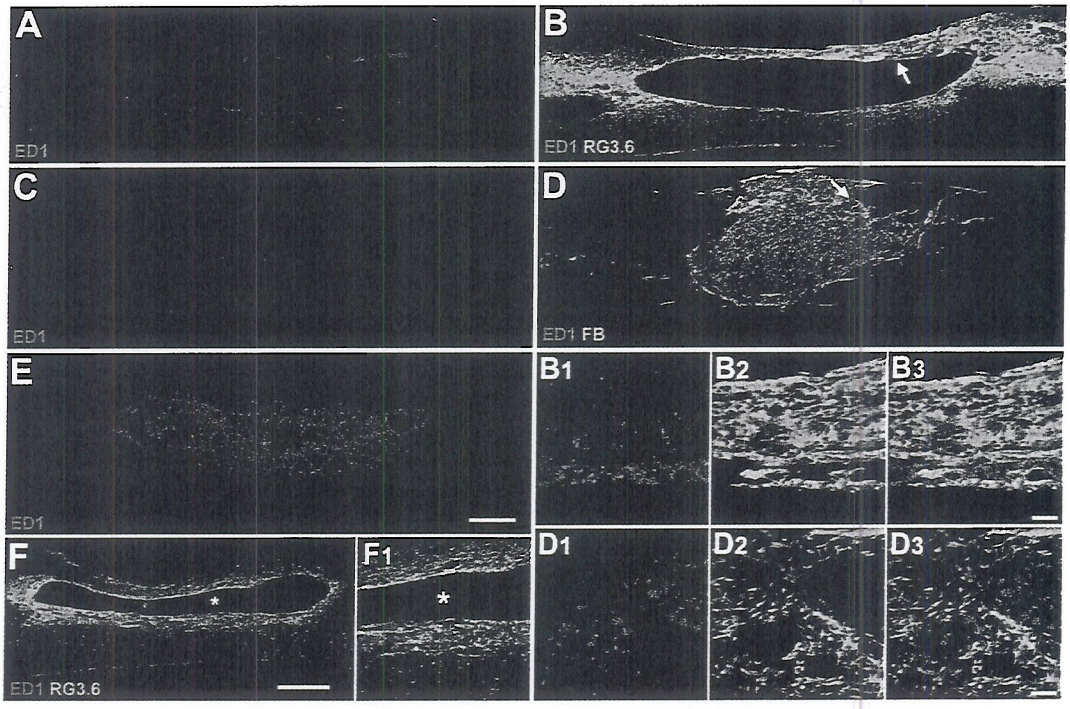

Fig. 8. Radial glia reduce macrophage accumulation at 6 weeks after spinal cord injury. ED1 staining in parasagittal sections of RG3.6 (A, B, and F), fibroblast (FB) (C and D), and control medium-treated groups (E). Twenty-four 10× images were tiled to cover the injury site using Zeiss LSM software. Panels B1–3 and D1–3 are higher power views of regions marked with arrows in panels B and D, respectively, that illustrate complementary distributions of the transplanted cells with the macrophages. Macrophages were much more prevalent in medium controls (E). A lateral section (F and enlarged in F1) of an RG3.6 transplant illustrates a higher density of macrophages in this region than the midline but in a complementary pattern with RG3.6 cells. Scale bar = 500 μM in A–F and 50 μM in other panels.

that received transplants of RG3.6 cells (Figs. 7G and H) or fibroblasts (Figs. 7I and J).

The walls of the cysts in RG3.6-transplanted rats showed some residual CSPG staining (Figs. 7B and C), which probably represents CSPGs other than NG2 that were barely detectable (Figs. 7G and H). Interestingly, rats that received transplants of fibroblasts also showed low levels of CSPG deposition. Measurement of staining confirmed reductions in CSPG that were most significant for NG2 (Figs. 7K–N). Thus, CSPG deposition alone cannot explain the functional recovery achieved with RG3.6 cells since similar reductions were achieved with fibroblast implants.

Given that macrophages are a major source of CSPGs in the injured spinal cord (Jones et al., 2002), the inhibition of

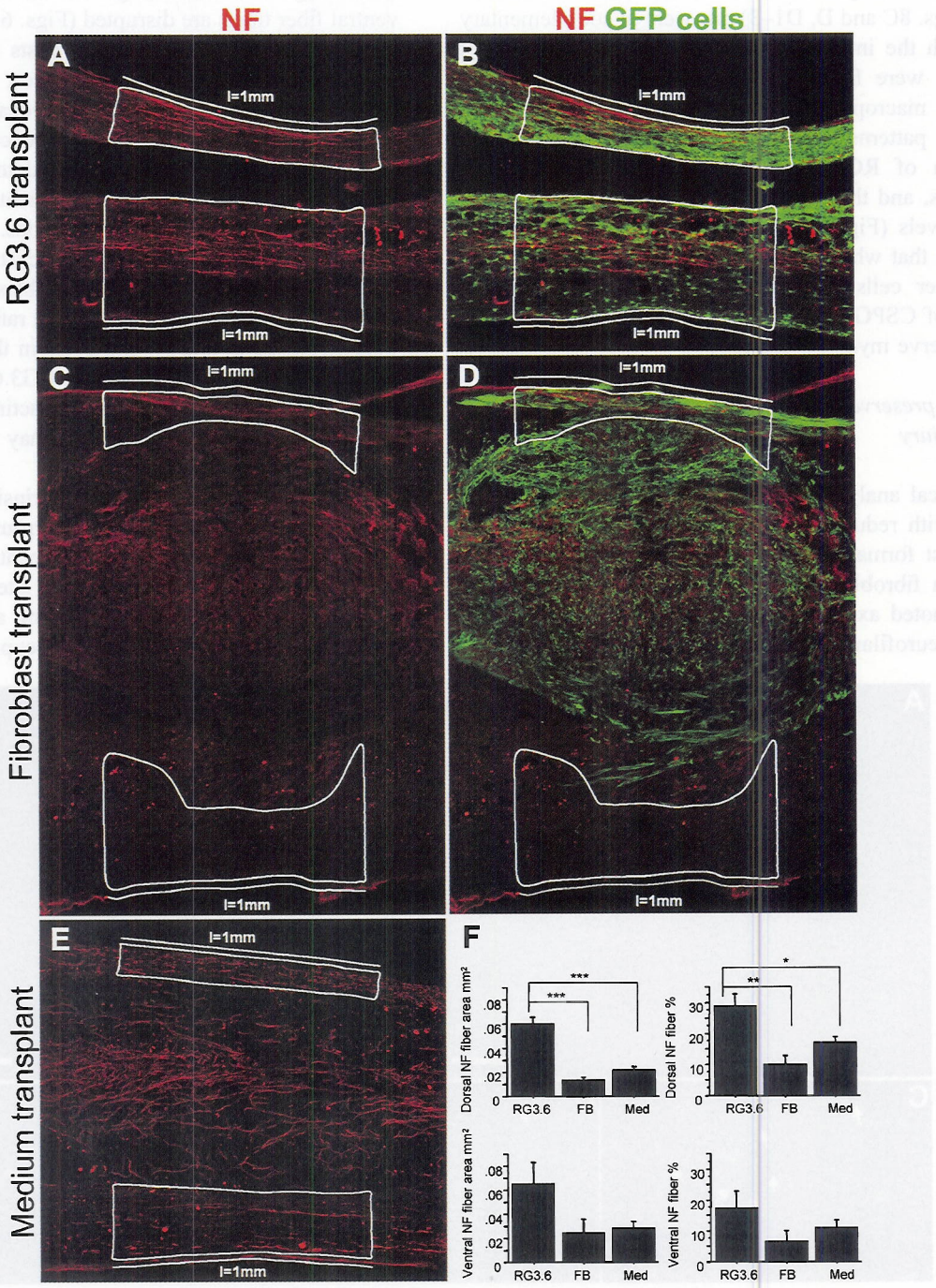

Fig. 9. RG3.6 cells promote white matter sparing. Sections stained for NF are shown for rats transplanted with RG3.6 (A and B), fibroblasts (C and D), and medium (E) 6 weeks after spinal cord injury. B and D are merged images. Spared dorsal and ventral fiber tracts were outlined (A–E) within 1 mm from the dorsal and ventral surfaces of the spinal cord in parasagittal sections and then measured using Zeiss confocal LSM software (F). Percentages of dorsal and ventral NF+ areas were normalized to the outlined areas (F). Data shown are means ± SEM with 3 rats per group (*$P < 0.05$, **$P < 0.01$, ***$P < 0.001$).

CSPG deposition in rats injected with RG3.6 cells raised the possibility that RG3.6 cells may interfere with macrophages. Immunostaining for activated macrophages with monoclonal antibody ED1 revealed very few reactive macrophages in rats treated with RG3.6 (Figs. 8A and B) or fibroblasts (Figs. 8C and D) in contrast to the large numbers detected in contused rats treated only with medium (Fig. 8E). The few macrophages that were detected in mid-sagittal sections in RG3.6-injected (Figs. 8A and B, B1–3) or fibroblast-injected (Figs. 8C and D, D1–3) rats were in complementary patterns with the implanted cells. In more lateral sections where there were fewer RG3.6 cells, there were greater numbers of macrophages than near the midline in non-overlapping patterns (Fig. 8F). The results suggest that implantation of RG3.6 cells can inhibit infiltration of macrophages, and this may explain the dramatic inhibition in CSPG levels (Fig. 7). The mutually exclusive patterns also suggest that where macrophages do infiltrate they can exclude other cells perhaps as a consequence of local deposition of CSPGs. The exclusion of macrophages may help to preserve myelin and axons.

RG3.6 cells preserve neurofilaments in spinal cord following injury

Histological analyses indicated that functional recovery correlated with reductions in macrophages and CSPG but not with cyst formation, which was observed with RG3.6 but not with fibroblast-treated rats. To determine whether RG3.6 promoted axon sparing or regrowth, we immunostained for neurofilament proteins (NF). By comparison to implants of fibroblasts or medium alone, spinal cords that received RG3.6 cells showed improved tissue architecture and NF alignment (Figs. 5, 6, 8, and 9). Rats treated with RG3.6 cells exhibited longitudinally-aligned NF closely apposed to the radial glia that were most prominent in regions containing RG3.6 cells (Figs. 5F,H–K and 9A,B). In contrast, rats treated with fibroblasts or medium alone exhibited thinner regions in the center of the injury site containing NF bundles (Figs. 9C–E) where the dorsal and ventral fiber tracts are disrupted (Figs. 6A, B, and G). There was little or no NF staining in cysts that formed in rats treated with RG3.6, but in these cases, NFs were abundant in regions where RG3.6 cells were located (Figs. 5E–I and 9A,B). Interestingly, some regions occupied by longitudinally-oriented RG3.6 cells appeared to lack myelin (Fig. 6F), although they were rich in oriented NF, which may represent spared or regrowing axons. In contrast, most fibroblast-treated rats did not form cysts but had disorganized NF intermingled with the fibroblasts in the injury site (Figs. 9C and D). In medium-treated rats, disorganized NFs were observed in and around cysts in the injury site (Figs. 5G and 9E). The lack of NF in RG3.6-treated cysts may reflect axonal preference for interacting with radial glia surrounding the cysts and thereby may increase the size of the dorsal and ventral fiber tracts.

RG3.6 cells identified by their intrinsic GFP fluorescence revealed that the implanted cells surrounded the injury site and were typically observed in adjacent white matter tracts and contiguous regions in the injury site (Figs. 5F and 9B). To analyze differences in NF staining among the different treatments, we measured areas occupied by NF in the

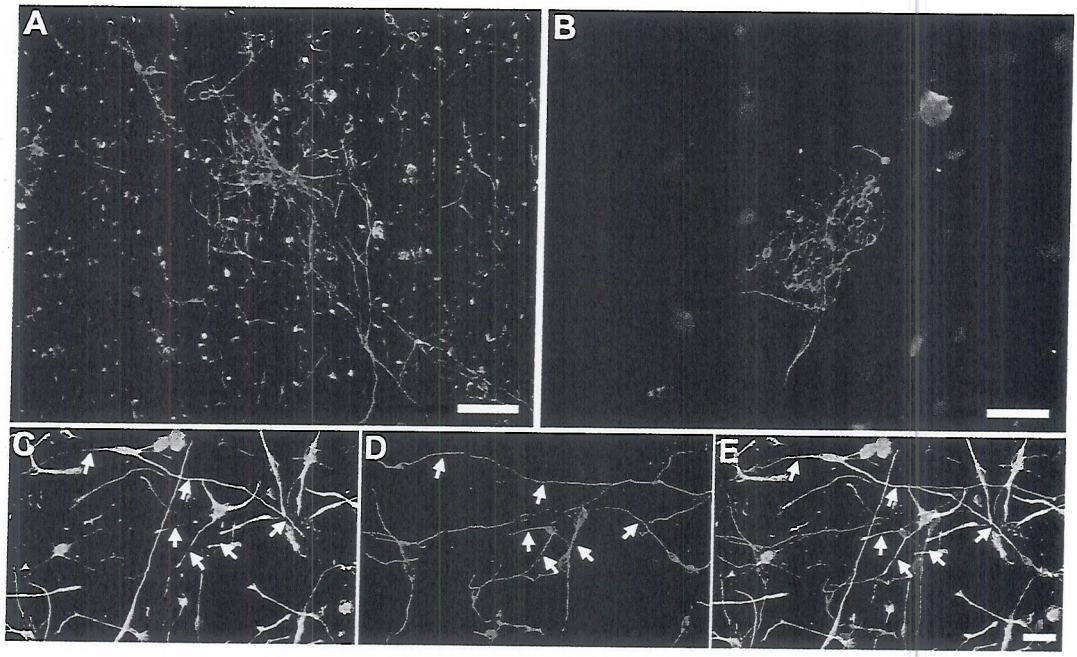

Fig. 10. Cocultures of cerebellar granule neurons on RG3.6 cells or fibroblasts. Aggregates of cerebellar granule neurons were grown on monolayers of RG3.6 (A and C–E) or GFP fibroblast (B). Immunostaining with TuJ1 antibody (red) revealed that neuronal fiber outgrowth was much more extensive on RG3.6 cells than on fibroblasts, and higher magnification views showed very close association of the neurites along the radial glial processes (arrows) that are seen in the overlay (E) of the RG3.6 cells (C) and the neurites (D). Scale bars = 50 μm in A and B, and 20 μm in E.

remnants of the fiber tracts around the injury site. In sagittal cryosections, areas occupied by NF+ cells in dorsal fiber tracts were statistically greater for RG3.6-treated rats than rats treated with fibroblasts or medium alone (Fig. 9). A similar trend was observed in ventral fiber tracts. The results indicate that NF staining was more organized and abundant in presumptive fiber tracts of rats implanted with RG3.6 than those treated with fibroblasts or medium alone.

The close coalignment of NF+ fibers with GFP+ radial glia and the increase in the area of NF+ staining suggest that RG3.6 radial glia may interact with axons and promote axonal growth. To test this hypothesis, we cultured granule cell neurons on monolayers of RG3.6 cells and fibroblasts. Granule neurons extended long processes on monolayers of RG3.6 cells but not on fibroblasts where they tended to associate with each other (Figs. 10A and B). The close association of the neurites along radial glial fibers suggests an interaction that can guide neurite growth along the radial glia (Figs. 10C–E). These results suggest that RG3.6 cells provide a favorable substrate for neuronal interaction that can support axonal outgrowth.

Discussion

The major findings of this study are that acutely following spinal cord contusion transplanted radial glia (1) form bridges that span across the contusion site and expand into spared spinal cord tissue, (2) suppress macrophage accumulation, formation of trabeculae, and deposition of CSPGs in the injury site, (3) promote the number and organization of NF around the injury site, and (4) promote functional recovery. Because radial glia differentiate in the adult spinal cord, we introduced v-myc into radial glia to retard their differentiation, which allowed many RG3.6 to persist as nestin+ elongated cells for extended periods of time in vivo. The strong and persistent expression of GFP in RG3.6 cells in vivo was particularly advantageous as it allowed unequivocal identification of the transplanted cells and their processes.

Previous studies demonstrated that embryonic neural tissue transplants can bridge across gaps or cysts in the spinal cord following trans-section or contusion that produced some functional improvement, probably acting by a variety of cellular and molecular mechanisms (Bregman, 1998; Jones et al., 2001; Schwab, 2002). Dissociated cells such as Schwann cells also have facilitated regrowth of axons and functional recovery in combination therapies, but they do not migrate into the CNS (Pearse et al., 2004). Thus it was of interest to isolate cells that can self-assemble bridges extending into spared rostral and caudal spinal cord without the need to provide additional devices for their assembly. However, to date, this has not been accomplished and there has been concern whether such a goal is practical (Geller and Fawcett, 2002). Our studies are the first to demonstrate that "bridging" of spinal cord lesions with radial glia is possible and is associated with functional recovery. Moreover, while other studies used delayed implants to increase graft survival (McDonald et al., 1999; Plant et al., 2003; Rosenzweig and McDonald, 2004), we obtained results with immediate injection that provides novel data on early effects of cell transplants during the first week following injury.

The mechanisms responsible for improved acute recovery after spinal cord contusion and transplantation of radial glia may be complex but appear to involve tissue protection. Behavioral scoring performed within the first week following injury showed significant improvement in rats transplanted with RG3.6 by comparison to rats that received fibroblasts or medium alone with increases in BBB scores of >2 points. These early responses (2–7 days after contusion) that persisted for several weeks cannot be explained by regeneration, which would take at least several weeks. Rather, it is most likely due to cellular and biochemical changes produced by the radial glia in and around the site of injury. Although we cannot rule out sprouting mechanisms that may contribute to recovery, like regeneration, they would be expected to require longer times than 1 week to promote functional recovery (Bareyre et al., 2004). The increases in NF staining and organization as well as in myelin preservation observed with RG3.6 cells suggest that radial glial transplantation preserved portions of dorsal and ventral fiber tracts following spinal cord injury. The robust migration of RG3.6 cells in the white matter is evident in the normal spinal cord (Fig. 3J) and RG3.6 cells promote axonal growth in vitro (Fig. 10). Radial glia also promote axonal growth during development (Brittis et al., 1995; Norris and Kalil, 1991). Thus, radial glial interactions with axons in vivo may be neuroprotective by inhibiting macrophage infiltration and may promote axonal growth by interacting with axons.

Unlike astrocytes that rapidly leave contusion sites or transform into GFAP+ reactive glia (Hoke and Silver, 1994), many of the radial glia that survive following transplantation are located surrounding the injury site. Radial glia also migrated into myelinated regions where they often coaligned longitudinally with axons (Hormigo et al., 2001b) (Figs. 5H,I and 9B) and thus may provide physical and metabolic support to protect axons from secondary injury. Like astroglia, radial glia express various transporters that can facilitate clearance of potentially excitotoxic chemicals including Ca^{++} and glutamate (Komuro and Rakic, 1998) that may protect neurons locally from secondary damage. Interestingly, radial glia suppressed deposition of CSPGs including NG2 in and around contusion sites. These complex proteoglycans have been shown to inhibit axonal growth in vitro (Grumet et al., 1996) and in vivo (Davies et al., 1997), and axonal regrowth is promoted by degrading CSPG with bacterial chondroitinase (Bradbury et al., 2002). Macrophages are a major source of CSPGs in injured spinal cord (Jones et al., 2002), and staining with ED1, which recognizes activated macrophages, was much lower in

contused rats that received RG3.6 and fibroblasts than medium controls (Fig. 8). Interestingly, when macrophages were detected, they were in a complementary pattern with RG3.6 cells, suggesting that radial glia inhibit macrophage accumulation and CSPG deposition, and reciprocally that radial glia migration may be restricted from regions occupied by activated macrophages. Thus, radial glia can dramatically influence the extracellular milieu in the spinal cord acutely following injury.

Olfactory ensheathing glia (OEG) have attracted considerable attention because they migrate in the adult spinal cord, form myelin, and promote axonal regeneration and functional recovery (Santos-Benito and Ramon-Cueto, 2003). A recent study indicated that transplantation of OEG cells 7 days after contusion improved axonal sparing/regeneration and hindlimb performance (Plant et al., 2003). Interestingly, BBB scores within the first week after transplant were higher with the OEG transplants than the controls suggesting axon sparing. Although detection of the OEG cells following transplantation was not performed, it will be interesting to know whether OEG cells can bridge the lesion site as observed for radial glia. The survival of OEG cells in contusion sites was better at 7 days rather than immediately following contusion (Plant et al., 2003). It is likely that radial glial survival in the injury site will also be improved by delayed transplantation. Indeed, transplantation of rats with neural differentiated mouse embryonic stem cells at 9 days after contusion promoted functional recovery (McDonald et al., 1999). These cells were highly polarized in vitro and many of them may be radial glia, consistent with their differentiation primarily into glia in vivo (McDonald et al., 1999).

Recent reports of transplantation of glia-restricted precursors (GRPs) into the spinal cord indicated that they differentiated primarily into glia (Han et al., 2004; Hill et al., 2004). When GRPs were injected into contusion sites within 20 min following injury, they exhibited little migration (Hill et al., 2004). We also found poor cell survival with cell transplants immediately following injury into the contusion site (K.H. and M.G., unpublished observations) and therefore developed a 3-point injection protocol adding two additional targets that are rostral and caudal to the injury site where the transplanted cells showed good survival and extensive migration (see Fig. 6, Materials and methods). One week after injury, transplantation of GRPs resulted in more extensive migration with the cells initially assuming elongated shapes in white matter (Han et al., 2004). A2B5 is a key marker for GRPs that is expressed on a subset of radial glia, and developmental studies suggest that GRPs are derived from radial glia (Li et al., 2004; Liu et al., 2002b). Thus, GRPs exhibit some similarities with radial glia, consistent with the idea that they may be derived from them (Li et al., 2004; Liu et al., 2002b). However, GRPs differentiate into glia, and it is unclear how they will affect recovery following spinal cord injury, considering that gliosis may be detrimental. It has been suggested that induction of cytokines that promote astrocytic differentiation are associated with spinal cord injury and may promote gliosis (Okano et al., 2003). Thus, it may be important to prevent or delay astrocytic differentiation of transplanted cells as we have done here with RG3.6 cells.

Marrow stromal cells (MSCs) in culture can express neural differentiation markers and their transplantation into the spinal cord 9 days after injury produced some improvement (1.3 points) in BBB scores (Hofstetter et al., 2002). MSCs tended to form strands adjacent to scar tissue that coaligned with nestin+, GFAP+, and NF+ staining, but their phenotype in vivo is unclear. MSC survival immediately following injury was very poor and did not result in any functional improvement in contrast to the results described here with RG3.6 (Figs. 5 and 6). MSCs represent a potential source of NSC but their ability to display beneficial properties needs to be examined further.

In contrast to radial glia that can bridge across spinal cord lesions, fibroblasts do not migrate into the CNS but have been used effectively to deliver soluble proteins such as neurotrophins (Tobias et al., 2003). Although fibroblasts may interfere with dural integrity (see Fig. 6), they may modify the local environment and improve recovery by providing certain growth factors and inhibiting macrophage infiltration. It is unlikely that acutely transplanted cells non-specifically inhibit macrophage infiltration in the injured spinal cord inasmuch as transplants of fetal spinal cord cells (Lemons et al., 1999), Schwann cells (Takami et al., 2002), olfactory ensheathing glia (Takami et al., 2002), and GRPs (Hill et al., 2004) did not result in suppression of CSPG deposition. It is more likely that certain cells including RG3.6 cells and dermal fibroblasts release specific factors that modulate the local environment. It is unclear whether the reductions in macrophages and CSPG staining associated with transplantation of RG3.6 cells and fibroblasts are due to common or different mechanisms. Interestingly, decorin, a proteoglycan that can modulate the activity of factors including TGFβ, suppressed accumulation of ED1+ cells following cerebral injury (Logan et al., 1999), and it was recently reported that decorin suppresses expression of several CSPGs in the injured spinal cord (Davies et al., 2004). It will therefore be interesting to determine whether radial glia and fibroblasts express decorin in vitro and in vivo following transplantation into spinal cord injury sites.

Whereas fibroblasts remained exclusively in the injury site following transplantation, radial glia migrated into spinal cord lesions and adjacent spared white matter but not towards the pial surface. Thus the migratory properties of radial glia suggest they may serve as particularly useful vehicles for local delivery of soluble factors such as neurotrophins. Although RG3.6 cells express levels of NGF and BDNF mRNAs that are not dramatically higher than in fibroblasts as detected by RT-PCR analyses, they have higher levels of NT3 (O.I., Y.-W.C., M.G., unpublished observations), suggesting that secretion of neurotrophins may be another beneficial aspect of RG3.6. However, additional studies are needed to

determine whether these or other growth factors are expressed in the spinal cord by transplants. Interestingly, the C17.2 cell line isolated from NSC also expressed NT3, and enhanced NT3 expression in these cells promoted recovery from spinal cord injury (Lu et al., 2003).

The ability of radial glia to interact with axons and migrate in white matter regions of intact and injured adult CNS (Hormigo et al., 2001b) suggests that these cells may be useful for other CNS disorders. In order to prevent radial glia from differentiating in vivo (Han et al., 2004; Hunter and Hatten, 1995), we introduced v-myc given its efficacy in preventing differentiation of C17.2 cells (Villa et al., 2000). Although we did not observe tumor formation with RG3.6, it may be important to explore other approaches to retain a radial glial phenotype without introduction of oncogenes. For example, neuregulins promote the radial glial phenotype (Schmid et al., 2003), and activation of this signaling pathway may be useful in maintaining radial glia in vivo. Finally, advances in cell technologies suggest that embryonic stem cells may be a plentiful source of cells that can be differentiated into radial glia (Liour and Yu, 2003).

Acknowledgments

We thank Dr. Evan Snyder for retrovirus, Drs. Joel Levine, Nathaniel Heintz, and Randall D. McKinnon for antibodies, Dr. Wise Young for advice, and Joanne Babiarz, Ryan Kirchoff, Jeffrey Massone, and Hock Ng for technical assistance. Supported by grants from NIH, New Jersey Commission on Spinal Cord Research, and Morton Cure Paralysis Fund.

References

Anthony, T.E., Klein, C., Fishell, G., Heintz, N., 2004. Radial glia serve as neuronal progenitors in all regions of the central nervous system. Neuron 41, 881–890.

Bareyre, F.M., Kerschensteiner, M., Raineteau, O., Mettenleiter, T.C., Weinmann, O., Schwab, M.E., 2004. The injured spinal cord spontaneously forms a new intraspinal circuit in adult rats. Nat. Neurosci. 7, 269–277.

Basso, D.M., Beattie, M.S., Bresnahan, J.C., 1996a. Graded histological and locomotor outcomes after spinal cord contusion using the NYU weight-drop device versus transection. Exp. Neurol. 139, 244–256.

Basso, D.M., Beattie, M.S., Bresnahan, J.C., Anderson, D.K., Faden, A.I., Gruner, J.A., Holford, T.R., Hsu, C.Y., Noble, L.J., Nockels, R., Perot, P.L., Salzman, S.K., Young, W., 1996b. MASCIS evaluation of open field locomotor scores: effects of experience and teamwork on reliability. Multicenter Animal Spinal Cord Injury Study. J. Neurotrauma 13, 343–359.

Beattie, M.S., Li, Q., Bresnahan, J.C., 2000. Cell death and plasticity after experimental spinal cord injury. Prog. Brain Res. 128, 9–21.

Bradbury, E.J., Moon, L.D., Popat, R.J., King, V.R., Bennett, G.S., Patel, P.N., Fawcett, J.W., McMahon, S.B., 2002. Chondroitinase ABC promotes functional recovery after spinal cord injury. Nature 416, 636–640.

Bregman, B.S., 1998. Regeneration in the spinal cord. Curr. Opin. Neurobiol. 8, 800–807.

Brittis, P.A., Lemmon, V., Rutishauser, U., Silver, J., 1995. Unique changes of ganglion cell growth cone behavior following cell adhesion molecule perturbations: a time-lapse study of the living retina. Mol. Cell Neurosci. 6, 433–449.

Cao, Q.L., Zhang, Y.P., Howard, R.M., Walters, W.M., Tsoulfas, P., Whittemore, S.R., 2001. Pluripotent stem cells engrafted into the normal or lesioned adult rat spinal cord are restricted to a glial lineage. Exp. Neurol. 167, 48–58.

Carson, F.L., 1997. Histotechnology: A Self-Instructional Text. ASCP Press, Chicago.

Constantini, S., Young, W., 1994. The effects of methypredniosolone and the ganglioside GM1 on acute spinal cord injury in rats. J. Neurosurg. 80, 97–111.

Davies, S.J., Fitch, M.T., Memberg, S.P., Hall, A.K., Raisman, G., Silver, J., 1997. Regeneration of adult axons in white matter tracts of the central nervous system. Nature 390, 680–683.

Davies, J.E., Tang, X., Denning, J.W., Archibald, S.J., Davies, S.J., 2004. Decorin suppresses neurocan, brevican, phosphacan and NG2 expression and promotes axon growth across adult rat spinal cord injuries. Eur. J. Neurosci. 19, 1226–1242.

Feng, L., Heintz, N., 1995. Differentiating neurons activate transcription of the brain lipid-binding protein gene in radial glia through a novel regulatory element. Development 121, 1719–1730.

Friedlander, D.R., Brittis, P., Sakurai, Y., Shif, B., Wirchansky, W., Fishell, G., Grumet, M., 1998. Generation of a radial-like glial cell line. J. Neurobiol. 37, 291–304.

Gage, F.H., 2000. Mammalian neural stem cells. Science 287, 1433–1438.

Geller, H.M., Fawcett, J.W., 2002. Building a bridge: engineering spinal cord repair. Exp. Neurol. 174, 125–136.

Gotz, M., Hartfuss, E., Malatesta, P., 2002. Radial glial cells as neuronal precursors: a new perspective on the correlation of morphology and lineage restriction in the developing cerebral cortex of mice. Brain Res. Bull. 57, 777–788.

Grill, R., Murai, K., Blesch, A., Gage, F.H., Tuszynski, M.H., 1997. Cellular delivery of neurotrophin-3 promotes corticospinal axonal growth and partial functional recovery after spinal cord injury. J. Neurosci. 17, 5560–5572.

Grumet, M., Flaccus, A., Margolis, R.U., 1993. Functional characterization of chondroitin sulfate proteoglycans of brain: Interactions with neurons and neural cell adhesion molecules. J. Cell Biol. 120, 815–824.

Grumet, M., Friedlander, D.R., Sakurai, T., 1996. Functions of brain chondroitin sulfate proteoglycans during development: Interactions with adhesion molecules. Perspect. Dev. Neurobiol. 3, 319–330.

Hafidi, A., Grumet, M., Sanes, D.H., 2004. In vitro analysis of mechanisms underlying age-dependent failure of axon regeneration. J. Comp. Neurol. 470, 80–92.

Han, S.S., Liu, Y., Tyler-Polsz, C., Rao, M.S., Fischer, I., 2004. Transplantation of glial-restricted precursor cells into the adult spinal cord: survival, glial-specific differentiation, and preferential migration in white matter. Glia 45, 1–16.

Hasegawa, K., Grumet, M., 2003. Trauma induces tumorigenesis of cells implanted into rat spinal cord. J. Neurosurg. 98, 1065–1071.

Hatten, M.E., 1993. The role of migration in central nervous system neuronal development. Curr. Opin. Neurobiol. 3, 38–44.

Hatten, M.E., Heintz, N., 1995. Mechanisms of neural patterning and specification in the developing cerebellum. Annu. Rev. Neurosci. 18, 385–408.

Hill, C.E., Beattie, M.S., Bresnahan, J.C., 2001. Degeneration and sprouting of identified descending supraspinal axons after contusive spinal cord injury in the rat. Exp. Neurol. 171, 153–169.

Hill, C.E., Proschel, C., Noble, M., Mayer-Proschel, M., Gensel, J.C., Beattie, M.S., Bresnahan, J.C., 2004. Acute transplantation of glial-restricted precursor cells into spinal cord contusion injuries: survival, differentiation, and effects on lesion environment and axonal regeneration. Exp. Neurol. 190, 289–310.

Hofstetter, C.P., Schwarz, E.J., Hess, D., Widenfalk, J., El Manira, A., Prockop, D.J., Olson, L., 2002. Marrow stromal cells form guiding

strands in the injured spinal cord and promote recovery. Proc. Natl. Acad. Sci. U. S. A. 99, 2199–2204.
Hoke, A., Silver, J., 1994. Heterogeneity among astrocytes in reactive gliosis. Perspect. Dev. Neurobiol. 2, 269–274.
Hormigo, A., Friedlander, D.R., Brittis, P.A., Zagzag, D., Grumet, M., 2001a. Reduced tumorigenicity of rat glioma cells in the brain when mediated by hygromycin phosphotransferase. J. Neurosurg. 94, 596–604.
Hormigo, A., McCarthy, M., Nothias, J.M., Hasegawa, K., Huang, W., Friedlander, D.R., Fischer, I., Fishell, G., Grumet, M., 2001b. Radial glial cell line C6-R integrates preferentially in adult white matter and facilitates migration of coimplanted neurons in vivo. Exp. Neurol. 168, 310–322.
Hunter, K.E., Hatten, M.E., 1995. Radial glial cell transformation to astrocytes is bidirectional: regulation by a diffusible factor in embryonic forebrain. Proc. Natl. Acad. Sci. U. S. A. 92, 2061–2065.
Ito, T., Suzuki, A., Okabe, M., Imai, E., Hori, M., 2001. Application of bone marrow-derived stem cells in experimental nephrology. Exp. Nephrol. 9, 444–450.
Jones, L.L., Oudega, M., Bunge, M.B., Tuszynski, M.H., 2001. Neurotrophic factors, cellular bridges and gene therapy for spinal cord injury. J. Physiol. 533, 83–89.
Jones, L.L., Yamaguchi, Y., Stallcup, W.B., Tuszynski, M.H., 2002. NG2 is a major chondroitin sulfate proteoglycan produced after spinal cord injury and is expressed by macrophages and oligodendrocyte progenitors. J. Neurosci. 22, 2792–2803.
Kim, J.H., Auerbach, J.M., Rodriguez-Gomez, J.A., Velasco, I., Gavin, D., Lumelsky, N., Lee, S.H., Nguyen, J., Sanchez-Pernaute, R., Bankiewicz, K., McKay, R., 2002. Dopamine neurons derived from embryonic stem cells function in an animal model of Parkinson's disease. Nature 418, 50–56.
Komuro, H., Rakic, P., 1998. Orchestration of neuronal migration by activity of ion channels, neurotransmitter receptors, and intracellular Ca2+ fluctuations. J. Neurobiol. 37, 110–130.
Lemons, M.L., Howland, D.R., Anderson, D.K., 1999. Chondroitin sulfate proteoglycan immunoreactivity increases following spinal cord injury and transplantation. Exp. Neurol. 160, 51–65.
Levine, J.M., Card, J.P., 1987. Light and electron microscopic localization of a cell surface antigen (NG2) in the rat cerebellum: association with smooth protoplasmic astrocytes. J. Neurosci. 7, 2711–2720.
Li, H., Babiarz, J., Woodbury, J., Kane-Goldsmith, N., Grumet, M., 2004. Spatiotemporal heterogeneity of CNS radial glial cells and their transition to restricted precursors. Dev. Biol. 271, 225–238.
Liour, S.S., Yu, R.K., 2003. Differentiation of radial glia-like cells from embryonic stem cells. Glia 42, 109–117.
Liu, Y., Kim, D., Himes, B.T., Chow, S.Y., Schallert, T., Murray, M., Tessler, A., Fischer, I., 1999. Transplants of fibroblasts genetically modified to express BDNF promote regeneration of adult rat rubrospinal axons and recovery of forelimb function. J. Neurosci. 19, 4370–4387.
Liu, Y., Himes, B.T., Murray, M., Tessler, A., Fischer, I., 2002a. Grafts of BDNF-producing fibroblasts rescue axotomized rubrospinal neurons and prevent their atrophy. Exp. Neurol. 178, 150–164.
Liu, Y., Wu, Y., Lee, J.C., Xue, H., Pevny, L.H., Kaprielian, Z., Rao, M.S., 2002b. Oligodendrocyte and astrocyte development in rodents: an in situ and immunohistological analysis during embryonic development. Glia 40, 25–43.
Logan, A., Baird, A., Berry, M., 1999. Decorin attenuates gliotic scar formation in the rat cerebral hemisphere. Exp. Neurol. 159, 504–510.
Lu, P., Jones, L.L., Snyder, E.Y., Tuszynski, M.H., 2003. Neural stem cells constitutively secrete neurotrophic factors and promote extensive host axonal growth after spinal cord injury. Exp. Neurol. 181, 115–129.
Luna, L.G., 1968. Manual of Histologic Staining Methods of the Armed Forces Institute of Pathology. McGraw-Hill Book Co., New York, pp. 203–304.
Mabie, P.C., Mehler, M.F., Marmur, R., Papavasiliou, A., Song, Q., Kessler, J.A., 1997. Bone morphogenetic proteins induce astroglial differentiation of oligodendroglial–astroglial progenitor cells. J. Neurosci. 17, 4112–4120.
McDonald, J.W., Liu, X.Z., Qu, Y., Liu, S., Mickey, S.K., Turetsky, D., Gottlieb, D.I., Choi, D.W., 1999. Transplanted embryonic stem cells survive, differentiate and promote recovery in injured rat spinal cord. Nat. Med. 5, 1410–1412.
McKay, R., 1997. Stem cells in the central nervous system. Science 276, 66–71.
Noctor, S.C., Flint, A.C., Weissman, T.A., Wong, W.S., Clinton, B.K., Kriegstein, A.R., 2002. Dividing precursor cells of the embryonic cortical ventricular zone have morphological and molecular characteristics of radial glia. J. Neurosci. 22, 3161–3173.
Norris, C.R., Kalil, K., 1991. Guidance of callosal axons by radial glia in the developing cerebral cortex. J. Neurosci. 11, 3481–3492.
Okano, H., Ogawa, Y., Nakamura, M., Kaneko, S., Iwanami, A., Toyama, Y., 2003. Transplantation of neural stem cells into the spinal cord after injury. Semin. Cell Dev. Biol. 14, 191–198.
Pearse, D.D., Pereira, F.C., Marcillo, A.E., Bates, M.L., Berrocal, Y.A., Filbin, M.T., Bunge, M.B., 2004. cAMP and Schwann cells promote axonal growth and functional recovery after spinal cord injury. Nat. Med. 10, 610–616.
Plant, G.W., Christensen, C.L., Oudega, M., Bunge, M.B., 2003. Delayed transplantation of olfactory ensheathing glia promotes sparing/regeneration of supraspinal axons in the contused adult rat spinal cord. J. Neurotrauma 20, 1–16.
Roonprapunt, C., Huang, W., Grill, R., Friedlander, D., Grumet, M., Chen, S., Schachner, M., Young, W., 2003. Soluble cell adhesion molecule L1-Fc promotes locomotor recovery in rats after spinal cord injury. J. Neurotrauma 20, 871–882.
Rosenzweig, E.S., McDonald, J.W., 2004. Rodent models for treatment of spinal cord injury: research trends and progress toward useful repair. Curr. Opin. Neurol. 17, 121–131.
Santos-Benito, F.F., Ramon-Cueto, A., 2003. Olfactory ensheathing glia transplantation: a therapy to promote repair in the mammalian central nervous system. Anat. Rec. 271B, 77–85.
Schmid, R.S., McGrath, B., Berechid, B.E., Boyles, B., Marchionni, M., Sestan, N., Anton, E.S., 2003. Neuregulin 1-erbB2 signaling is required for the establishment of radial glia and their transformation into astrocytes in cerebral cortex. Proc. Natl. Acad. Sci. U. S. A. 100, 4251–4256.
Schwab, M.E., 2002. Repairing the injured spinal cord. Science 295, 1029–1031.
Silver, J., Miller, J.H., 2004. Regeneration beyond the glial scar. Nat. Rev. Neurosci. 5, 146–156.
Takahashi, J., Palmer, T.D., Gage, F.H., 1999. Retinoic acid and neurotrophins collaborate to regulate neurogenesis in adult-derived neural stem cell cultures. J. Neurobiol. 38, 65–81.
Takami, T., Oudega, M., Bates, M.L., Wood, P.M., Kleitman, N., Bunge, M.B., 2002. Schwann cell but not olfactory ensheathing glia transplants improve hindlimb locomotor performance in the moderately contused adult rat thoracic spinal cord. J. Neurosci. 22, 6670–6681.
Tobias, C.A., Shumsky, J.S., Shibata, M., Tuszynski, M.H., Fischer, I., Tessler, A., Murray, M., 2003. Delayed grafting of BDNF and NT-3 producing fibroblasts into the injured spinal cord stimulates sprouting, partially rescues axotomized red nucleus neurons from loss and atrophy, and provides limited regeneration. Exp. Neurol. 184, 97–113.
Tuszynski, M.H., Peterson, D.A., Ray, J., Baird, A., Nakahara, Y., Gage, F.H., 1994. Fibroblasts genetically modified to produce nerve growth factor induce robust neuritic ingrowth after grafting to the spinal cord. Exp. Neurol. 126, 1–14.
Tuszynski, M.H., Gabriel, K., Gage, F.H., Suhr, S., Meyer, S., Rosetti, A., 1996. Nerve growth factor delivery by gene transfer induces differential outgrowth of sensory, motor, and noradrenergic neurites after adult spinal cord injury. Exp. Neurol. 137, 157–173.
Villa, A., Snyder, E.Y., Vescovi, A., Martinez-Serrano, A., 2000. Establishment and properties of a growth factor-dependent, perpetual neural stem cell line from the human CNS. Exp. Neurol. 161, 67–84.